INTERNATIONAL JOURNAL FOR NUMERICAL METHODS IN FLUIDS, VOL. 6, 445–458 (1986)

SYNTHESIS OF THERMAL EFFECTS IN MISALIGNED HYDRODYNAMIC JOURNAL BEARINGS

J. O. MEDWELL* AND D. T. GETHIN*

Department of Mechanical Engineering, University College of Swansea, Singleton Park, Swansea 5A2 8PP, U.K.

SUMMARY

The analysis presented herein deals with the evaluation of pressure and temperature fields which are generated in thin fluid films of varying thickness. The particular problem of a misaligned journal bearing has been studied by solving simultaneously the Reynolds and energy equations, which also include the effects of viscous dissipation and the variation of fluid viscosity with temperature.

The method has been used to predict pressure and temperature fields as well as global performance parameters for a typical journal bearing operation.

INTRODUCTION

There are a large number of practical flow problems which involve the movement of a thin fluid film between two surfaces in relative motion. If the surfaces are inclined then a pressure field is generated in the film and it is this capacity for supporting a load that forms the basis of hydrodynamic lubrication. A common engineering artefact which exploits this principle is the cylindrical bore journal bearing in which a loaded shaft (or journal) rotates in a metallic bush that is fed continuously by a lubricating fluid. Under ideal operating conditions the longitudinal axes of both shaft and bush are parallel, although displaced eccentrically. This gives rise to a thin converging fluid film (see Figure 1(a)) which generates a pressure field and forms the load carrying portion of the bearing.

Often journal bearings operate in a misaligned mode where the shaft and bush axes are inclined to each other, this occuring most commonly in the plane in which the shaft is loaded (i.e. in the direction indicated by W in Figure 1(a), and is usually due to the flexure of the shaft). Consequently the resulting pressure and temperature fields in the lubricant film will be distorted, with the maximum pressure and temperature being significantly higher than in the aligned case. In many instances the latter quantity, which depends on the viscous dissipation in the lubricant film, is the limiting parameter on the range of bearing operation, and therefore the designer must have a method at his disposal for its estimation.

Although many procedures exist for the calculation of bearing characteristics for aligned cases, little information is available for the 'off design' operation referred to above. Some work exists for isothermal cases,[1–3] and recently further work[4] has endeavoured to account for thermal effects by including dissipation due to shearing action in the thin films.

With the exception of the work described in Reference 4, the major shortcoming of most approaches is that they ignore the temperature dependency of the lubricant viscosity, and that

*Lecturers in Mechanical Engineering

0271–2091/86/070445–14$07.00

Received 18 January 1986
Revised 18 January 1986

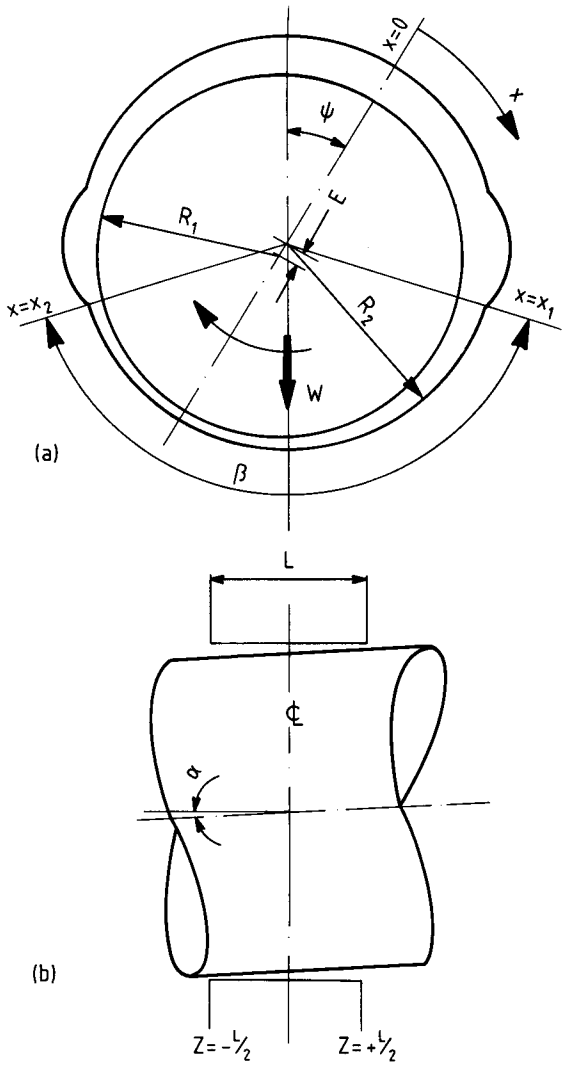

Figure 1. Bearing notation

they are addressed to a bearing which is supplied with lubricant at a point close to the maximum film thickness—a configuration which is not used extensively in practice since it may not allow birotational motion of the shaft. By adopting a single feed point, the analysis is simplified considerably, since it is unnecessary to update the film thickness profile during the mildly iterative (i.e. convergence in a few iterations) calculation as it is with a twin axial groove geometry for example (see Figure 1(a)). Indeed it is the necessity to update the film profile which renders the solution strongly iterative in nature. This arises since the journal will assume a final position in the bearing which depends on the applied loading.

The present paper illustrates a method for analysing the behaviour of a bearing fed by two axial grooves, as well as linking the fluid properties of the film to local film temperature to give a complete thermohydrodynamic solution to the problem. This involves, basically, the simultaneous solution of the Reynolds and energy equations using finite difference methodology.

Because, in practice, misalignment in high load, high speed operation causes many bearing failures, the analysis employed here has been adapted for turbulent lubricant films.

ANALYSIS

The Reynolds equation for a steadily loaded journal bearing of finite width may be written as

$$\frac{\partial}{\partial x}\left(\frac{h^3(x,z)}{\eta}G_x\frac{\partial p}{\partial x}\right)+\frac{\partial}{\partial z}\left(\frac{h^3(x,z)}{\eta}G_z\frac{\partial p}{\partial z}\right)=\frac{U}{2}\frac{\partial h(x,z)}{\partial x}, \tag{1}$$

where G_x and G_z are included to account for the augmented exchange or transport properties associated with turbulent motion.

An energy equation may be derived in which the variation of the mean temperature of the lubricant is described by a balance of the generated heat with that convected away in the film. Hence any cross-film or streamwise conduction effects are neglected, giving rise to the so-called adiabatic condition—a good approximation for thick films operating under turbulent conditions. The temperature of the lubricant film at any point (x, z) can be represented by a mean value T_m and appears in the energy equation in the following manner:

$$\rho C_p\left\{\left(\frac{Uh(x,z)}{2}-\frac{h^3(x,z)}{\eta}G_x\right)\frac{\partial T_m}{\partial x}-\frac{h^3(x,z)}{\eta}G_z\frac{\partial p}{\partial z}\frac{\partial T_m}{\partial z}\right\}$$
$$=-\tau_c U+\frac{h^3(x,z)}{\eta}\left\{G_x\left(\frac{\partial p}{\partial x}\right)^2+G_z\left(\frac{\partial p}{\partial z}\right)^2\right\}, \tag{2}$$

where

$$\frac{h(x,z)\tau_c}{\eta U}=1+0{\cdot}0012\left(\frac{Uh(x,z)}{\nu}\right)^{0{\cdot}94}. \tag{3}$$

The domains over which equations (1)–(3) give a complete description of the physical occurences are shown in Figures 1(a) and 1(b), together with other relevant geometric data required for the solution of the aforementioned equations. First the local lubricant film thickness under the misaligned conditions must be expressed. This may be done either by assuming (as did Asanabe *et al.*[1]) that the misalignment takes place along the diameter connecting the positions of maximum and minimum film thicknesses or, more realistically, along the load line. Hence

$$h(x,z)=(R_1-R_2)\left\{1+\varepsilon\cos\left(\frac{x}{R_1}-\psi\right)\right\}-\alpha z\cos\frac{x}{R_1}, \tag{4}$$

where the midplane eccentricity ratio

$$\varepsilon=\frac{E}{R_2-R_1}.$$

To complete the statement of the problem, the boundary conditions of the oil-film distribution and the temperature fields must be described. For the solution of the Reynolds equation, the boundary conditions are

$$p=0 \text{ at } x=x_1 \text{ and } x=x_2,$$

$$p=0 \text{ at } z=\pm\frac{L}{2},$$

$$p=0 \text{ when } p<0.$$

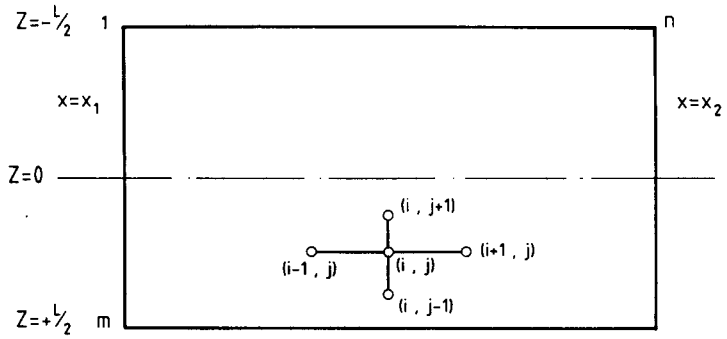

Figure 2. Finite difference representation for lubricant film

The boundary equations for the solution of the energy equation are

$$T_m = T_{inlet} \text{ at } x = x_1$$

and

$$\frac{\partial T_m}{\partial z} = 0 \text{ at } z = +\frac{L}{2}.$$

In the solution procedure, T_{inlet} will be specified, and the second boundary condition infers that, immediately at the edge of the bearing where the lubricant is thickest, no further heat is convected from the film axially.

Numerical solution procedure

The simultaneous solution of the Reynolds and energy equations requires that they be cast in finite difference form using the grid system shown in Figure 2. Thus the pressure equation may be expressed as

$$p_{i,j} = ap_{i,j+1} + bp_{i,j-1} + cp_{i+1,j} + dp_{i-1,j} + \Omega, \tag{5}$$

where a, b, c and d are parameters which are listed in Appendix I, and Ω represents the film thickness variation.

The finite difference form of the energy equation expresses the temperatures as

$$T_{i,j+1} = T_{i,j-1} + e\{T_{i+1,j} - T_{i-1,j}\} + \Phi, \tag{6}$$

where Φ represents the dissipation function and e is a further constant (see Appendix I).

The corresponding boundary conditions become, for pressure

$$\begin{aligned} &p_{i,j} = 0, \quad i = 1,\ldots,n; \quad j = 1,m, \\ &p_{i,j} = 0, \quad i = 1,n; \qquad j = 1,\ldots,m, \\ &p_{i,j} = 0, \quad \text{if} \quad p_{i,j} < 0, \end{aligned}$$

and for temperature

$$\begin{aligned} &T_{i,j} = T_{inlet}, \quad i = 1; \quad j = 1,\ldots,m, \\ &T_{i,j} = T_{i,j-1}, \quad i = 1,\ldots,n; \quad j = m. \end{aligned}$$

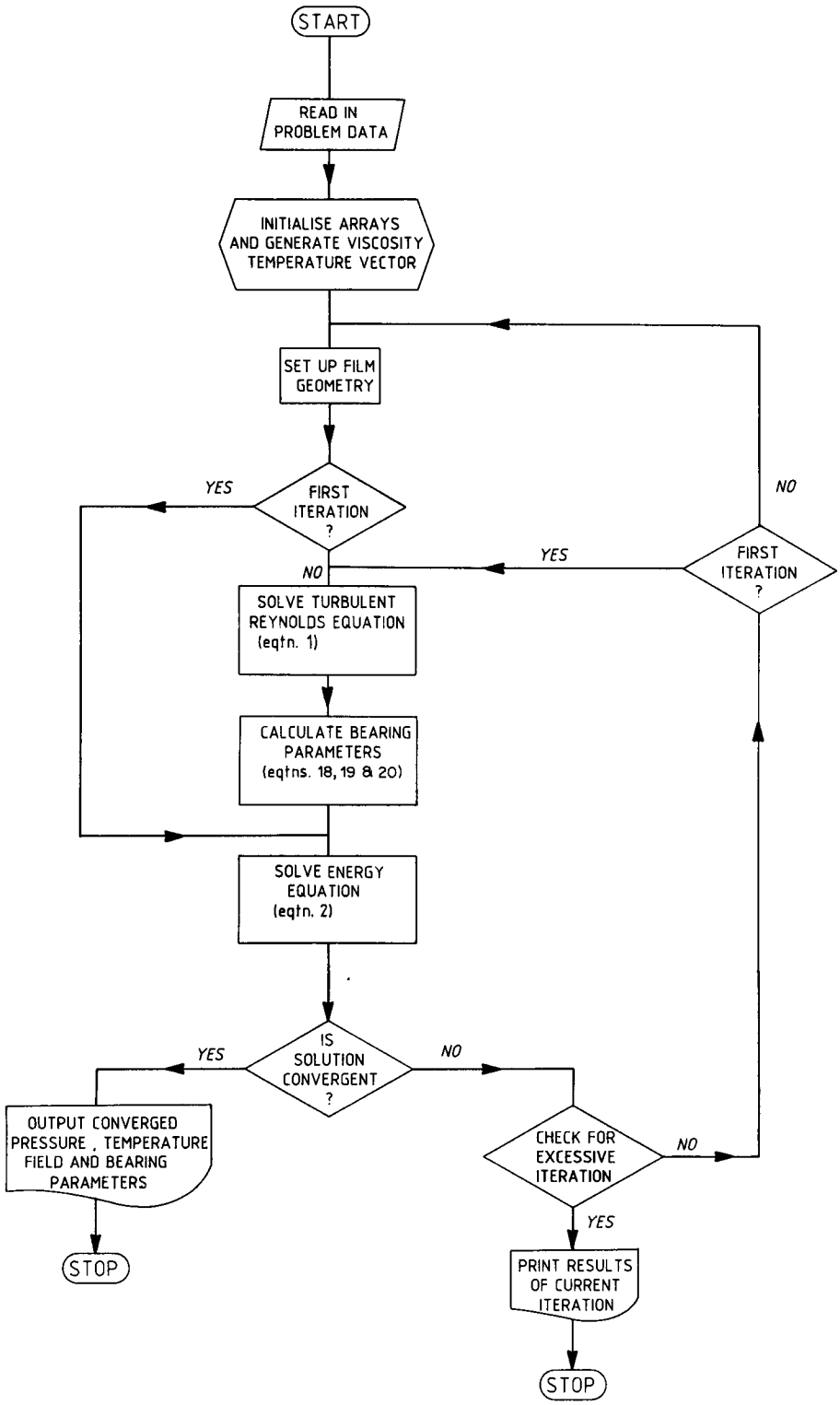

Figure 3. Flow diagram for solution procedure

The solution of the equations also requires the specification of the turbulence parameters which, following Ng and Pan,[5] are

$$\frac{1}{G_x} = 12 + 0{\cdot}0013\left[\frac{h(x,z)U}{\nu}\right]^{0{\cdot}9} \tag{7}$$

$$\frac{1}{G_z} = 12 + 0{\cdot}0043\left[\frac{h(x,z)U}{\nu}\right]^{0{\cdot}96} \tag{8}$$

Only the lubricant kinematic viscosity is assumed to be temperature dependent, and its variation is given by the Walther equation, i.e.

$$\log_{10}\{\log_{10}(\nu + 0{\cdot}6)\} = M \log_{10} T + B \tag{9}$$

The main sequences of the solution process may now be summarized as follows:

1. The bearing geometry (i.e. radii and width), operating speed, inlet temperature and midplane eccentricity ratio are selected. For the bearing which has two axial oil grooves in the horizontal plane the effective bearing arc is reduced and, for the case considered here, the partial arc is assigned the value of $8\pi/9$ radians.
2. An arbitrary value of attitude angle is chosen and the lubricant film thickness geometry field determined.
3. The viscosity–temperature array of the lubricant to be used is generated.
4. The energy equation is solved for Couette flow, i.e.

$$\frac{\partial p}{\partial x} \quad \text{and} \quad \frac{\partial p}{\partial z} = 0 \tag{10}$$

   to give an approximate temperature field.
5. This field is used to obtain the values of the lubricant properties for substitution into the Reynolds equation, which is then solved by a Gauss–Seidel iterative procedure to yield the pressure field.
6. A new attitude angle is evaluated from the pressure field and used to update the film thickness geometry.
7. The pressure gradient vectors are determined and used in the energy equation to calculate a new temperature field.
8. Steps (5) to (7) are repeated until a converged pressure field is obtaind.
9. Final bearing characteristics such as pressure and temperature fields, load, attitude angle and power loss are calculated. The relevant equations for their determination are given in Appendix II and Figure 3 gives the appropriate computer flow chart.

RESULTS AND DISCUSSION

One of the main objectives of this investigation (as stated earlier) is to provide a method for predicting temperature variations in a high-speed misaligned lubricant film and its consequent effect on the load-carrying capacity and power loss. To achieve this, the previously developed model has been applied to a journal bearing that had a bush of length and radius 36·8 mm with a clearance ratio $(R_2 - R_1)/R_1$ of 0·004. The lubricant used was Shell Tellus 27 which has a density of 860 kg/m^3 and a specific heat of 2000 J/kgK, which were assumed to be constant. The temperature dependence of the lubricant viscosity is obtained by assigning values of $M = -3.878$ and $B = 9{\cdot}85$ in the Walther equation (9). For this set of numerical experiments

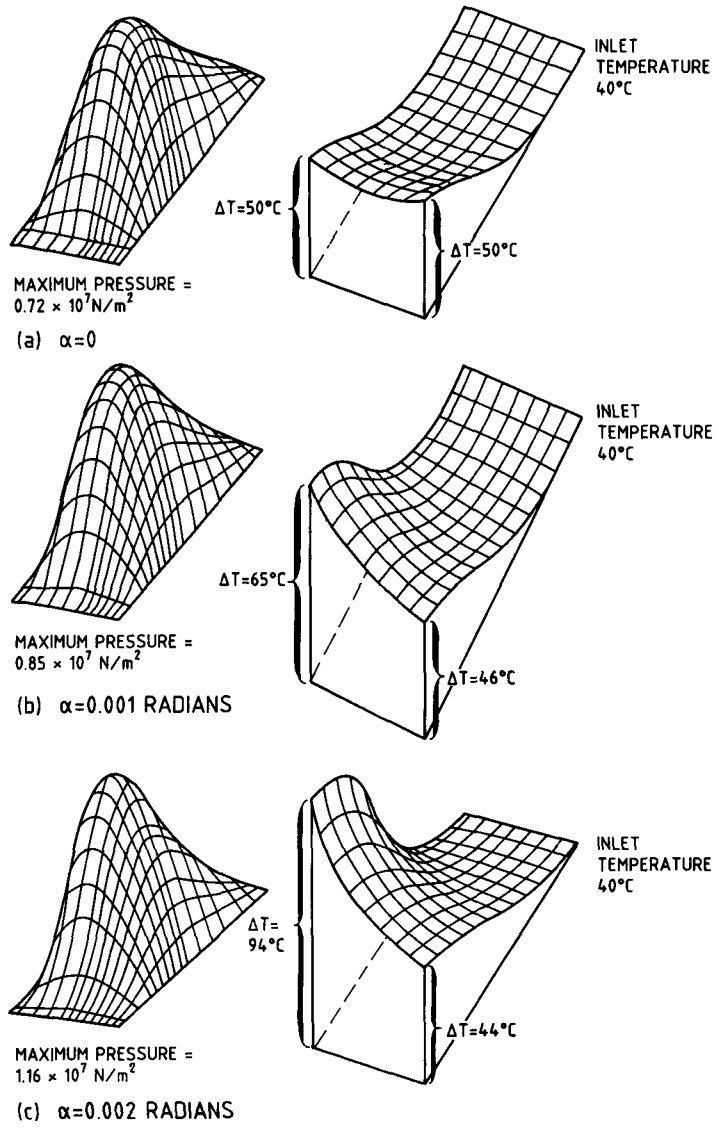

Figure 4. Bearing pressure and temperature fields: shaft speed = 40,000 Rev min^{-1}

the bearing shaft was assigned a rotational speed of 40,000 rev min^{-1} with a centre-line eccentricity ratio of 0·65.

The overall distortions of the lubricant film pressure and temperature fields are depicted pictorially in Figures 4(a), (b) and (c) for shaft inclinations of 0, 0·001 and 0·002 radians, respectively.

Generally, for a shaft that is constrained to misalign in the direction of the applied load, the peak pressure does not move in a streamwise direction, although increasing misalignment reduces slightly the extent of the cavitated region (or area of subzero pressure). However, the temperature increases continuously along the streamwise length of the film with the most rapid increases associated with the largest pressure gradients in the film.

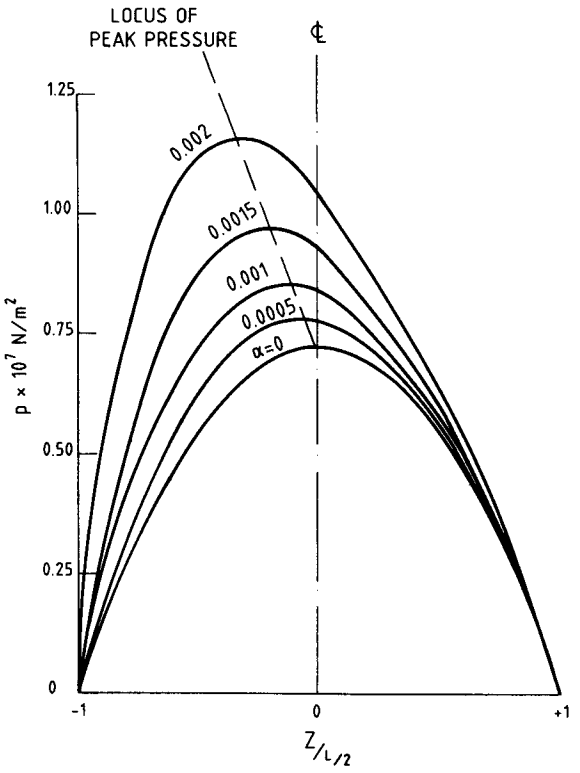

Figure 5. Peak pressure distributions for varying inclination: shaft speed = 40,000 Rev min^{-1}, $\varepsilon = 0{\cdot}65$, inlet temperature = 40° C

The axial variations of pressure and temperature, where the maximum values of these quantities occur, are shown in Figures 5 and 6. The circumferential positions at which peak pressures and temperatures are generated do not coincide for the cases considered here. Generally the maximum pressure is located at a position some 60 per cent of the arc length (β) from the main supply inlet. However, the maximum temperatures, because of the continued heat dissipation in the lubricant film, occur near to the onset of cavitation.

The results for the misalignment displayed in Figures 4(a), (b) and (c) are limited by the eccentricity ratio. To avoid surface contact between the shaft and bush when considering higher values of misalignment, the eccentricity ratio has to be reduced. This has the initial consequence of reducing the length of the cavitated zone in the partial arc film, permitting a fuller film to be established. However, the increased misalignment reduces further the minimum value of the lubricant film thickness while moving its position nearer to the upstream location. This enables cooler lubricant to flow into the regions downstream of the minimum clearance location. The cumulative effect of this is shown in Figure 7, where lines of constant lubricant temperature have been drawn to provide an isotherm map, thus showing that a distinctive 'hot spot' has been generated.

Some global performances for a misaligned bearing are shown in Figures 8 and 9 for an eccentricity ratio of 0·65. The isothermal solution, which is based on a constant lubricant temperature equal to that of inlet (i.e. 40° C), as expected, predicts far greater load and power losses than the full thermohydrodynamic solution. A further numerical experiment was carried out where the power loss computed using the thermohydrodynamic solution is used in a simple

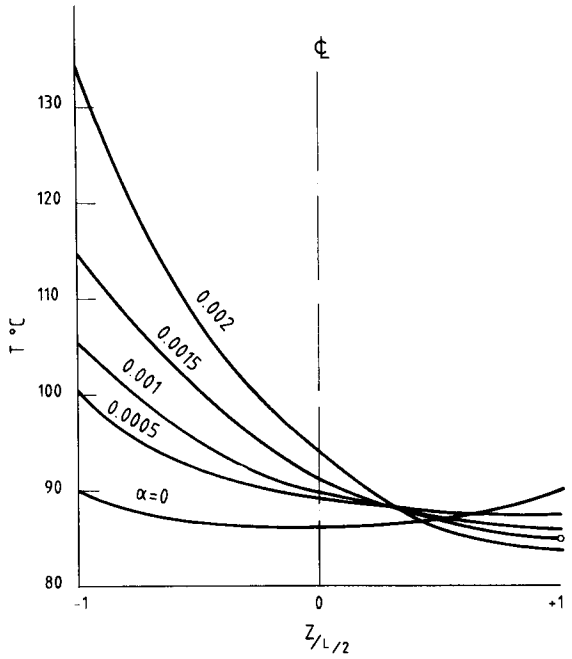

Figure 6. Axial maximum temperature distributions: shaft speed = 40,000 Rev min^{-1}, $\varepsilon = 0{\cdot}65$, inlet temperature = 40° C

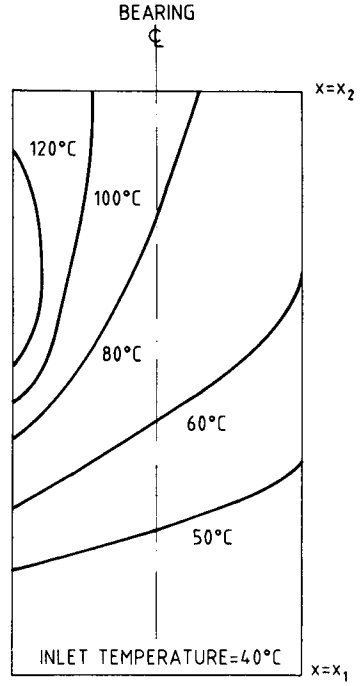

Figure 7. Bearing isotherms: shaft speed = 40,000 Rev min^{-1}, $\varepsilon = 0{\cdot}5$, $\alpha = 0{\cdot}0035$ Rev min

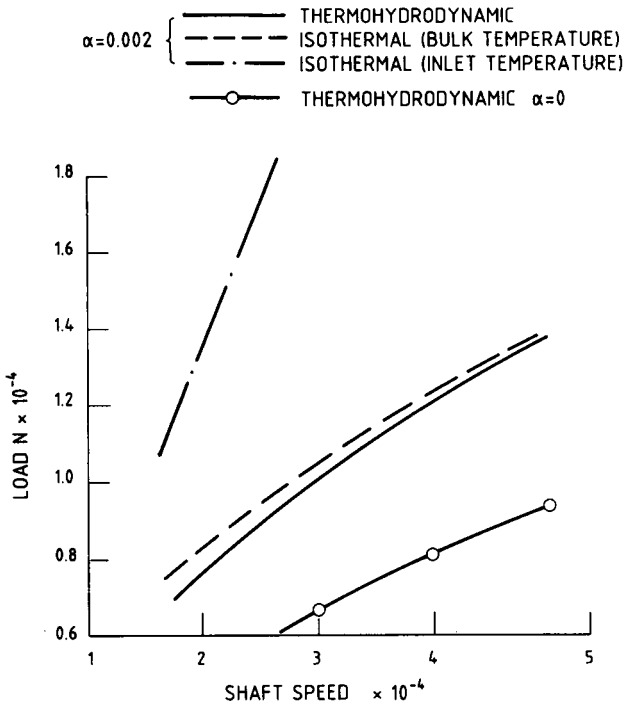

Figure 8. Variation of load capacity with bearing speed: $\varepsilon = 0{\cdot}65$, inlet temperature = 40° C

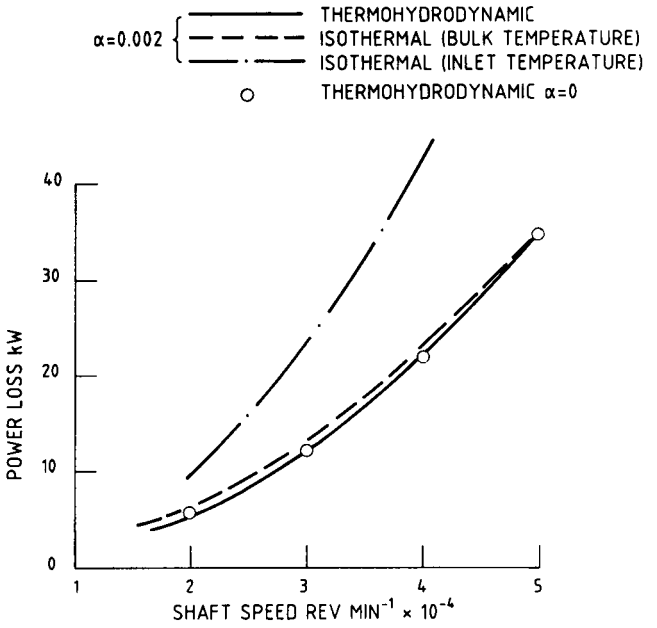

Figure 9. Variation of power loss with bearing speed: $\varepsilon = 0{\cdot}65$, inlet temperature = 40° C

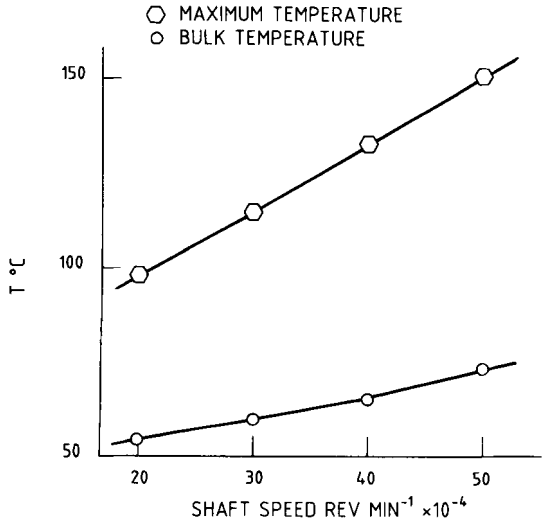

Figure 10. Variation of maximum and bulk temperatures with bearing speed: $\alpha = 0{\cdot}002$ radians, $\varepsilon = 0{\cdot}65$, inlet temperature = 40° C

energy balance, together with the predicted lubricant flow, to estimate the bulk lubricant temperature. This is equivalent to the sump temperature that would be monitored in situations where a bearing is likely to be highly stressed. If this temperature is used in the isothermal procedure, then the load and power loss characteristics compare closely with the thermo-hydrodynamic solution. The results of the aligned case are also included in the Figures where it can be seen that for a fixed eccentricity ratio, misalignment has significantly increased the load-carrying capacity only of the bearing. This is a consequence of the high peak pressures generated by misalignment, which more than offset the reduction in lubricant viscosity brought about by the accompanying increased temperatures. However, it should be pointed out that the increase in load carrying capacity is based on the midplane eccentricity ratio and is not in conflict, therefore, with the conclusions of other workers[1,6] since their contention of a reduction in load carrying capacity is based on minimum film thickness. In reality, the journal would position itself within the bush so as to react to the applied loading exactly.

Finally the maximum and bulk lubricant temperature variations with speed for a misalignment of 0·002 radians and an eccentricity of 0·65 are shown in Figure 10. It can be seen that although the bulk temperatures exhibit modest rises over the inlet lubricant temperature, the maximum temperatures generated are dangerously high and would certainly be a limiting parameter in such a bearing operation.

CONCLUSIONS

A procedure has been presented for the estimation of bearing performance in both normal mode operation and in off-design conditions.

One of the main features of the method is that the positions of the shaft relative to the bearing bush is not restricted by the solution method, which also accounts fully for the energy generated in the form of heat in the film.

It has been demonstrated that it is possible to predict distortions in the pressure and temperature field for misalignment of the shaft. Under such conditions, dangerously high temperatures, which are a frequent cause of bearing failure, can be encountered.

NOMENCLATURE

B	Constant defined in the Walther equation
C_p	Specific heat of lubricant
E	Eccentricity
G_x	Turbulence parameter (see equation (7))
G_z	Turbulence parameter (see equation (8))
H	Bearing power loss
L	Bearing length
M	Constant defined in the Walther equation
p	Local lubricant pressure
P	Component of load along line of centres
R_1	Radius of shaft
R_2	Radius of bush
T_m	Local mean temperature of lubricant
U	Surface velocity of the shaft
V	Component of load perpendicular to line of centres
W	Total bearing load
$h(x, z)$	Local lubricant film thickness
x	Circumferential distance measured from position of maximum clearance.
z	Axial distance measured from midplane of bearing
α	Angle of shaft misalignment
β	Length of lubricant partial arc
ε	Eccentricity measured on midplane of bearing
η	Absolute lubricant viscocity
ν	Lubricant kinematic viscosity
ρ	Lubricant density
τ_c	Couette shear stress
ψ	Attitude angle
Δ	Mesh size in finite difference scheme

Suffixes

i	nodal number in x direction
j	nodal number in z direction
1	indicates lubricant film commencement
2	indicates lubricant film end

a, b, c, d, e, Φ and Ω are constants used in finite difference equations as defined in the Appendix. Other quantities are defined as and when they occur.

APPENDIX I

The parameters, film thickness variation terms and dissipation function that appear in equations (5) and (6) are listed below:

$$a = \frac{\Delta_i^2 \Delta_j}{2h^3(x,z)(\Delta_i^2 G_x + \Delta_j^2 G_z)} \left\{ \frac{h^3(x,z)}{\Delta_j} G_x + \frac{h^2(x,z)}{2} \left[\frac{\partial h(x,z)}{\partial x} 3G_x + \frac{\partial G_x}{\partial x} h(x,z) \right] \right\}, \tag{11}$$

$$b=\frac{\Delta_i^2\Delta_j}{2h^3(x,z)(\Delta_i^2G_x+\Delta_j^2G_z)}\left\{\frac{h^3(x,z)}{\Delta_j}G_x-\frac{h^2(x,z)}{2}\left[\frac{\partial h(x,z)}{\partial x}3G_x+\frac{\partial G_x}{\partial x}h(x,z)\right]\right\}, \tag{12}$$

$$c=\frac{\Delta_i\Delta_j^2}{2h^3(x,z)(\Delta_i^2G_x+\Delta_j^2G_z)}\left\{\frac{h^3(x,z)}{\Delta_i}G_z+\frac{h^2(x,z)}{2}\left[\frac{\partial h(x,z)}{\partial z}3G_z+\frac{\partial G_z}{\partial z}h(x,z)\right]\right\}, \tag{13}$$

$$d=\frac{\Delta_i\Delta_j^2}{2h^3(x,z)(\Delta_i^2G_x+\Delta_j^2G_z)}\left\{\frac{h^3(x,z)}{\Delta_i}G_z-\frac{h^2(x,z)}{2}\left[\frac{\partial h(x,z)}{\partial z}3G_z+\frac{\partial G_z}{\partial z}h(x,z)\right]\right\}, \tag{14}$$

$$e=\frac{h^2(x,z)G_z\dfrac{\partial p}{\partial z}\Delta_j}{v\left[\dfrac{\rho U}{2}-\dfrac{G_x}{v}\right]\dfrac{\partial p}{\partial z}\Delta_i}, \tag{15}$$

$$\Omega=-\frac{v\Delta_i^2\Delta_j^2\rho U}{4h^3(x,z)(\Delta_i^2G_x+\Delta_j^2G_z)}\frac{\partial h(x,z)}{\partial x}, \tag{16}$$

$$\Phi=\frac{2\Delta_j}{C_ph(x,z)\left[\dfrac{U\rho}{2}-\dfrac{G_x}{v}\dfrac{\partial p}{\partial x}\right]}\left\{\frac{h^3(x,z)}{v\rho}\left[G_x\left(\frac{\partial p}{\partial x}\right)^2+G_z\left(\frac{\partial p}{\partial z}\right)^2\right]-\tau_cU\right\} \tag{17}$$

APPENDIX II

Figure 3 illustrates the main features of the computer program that was developed for the solution procedure described earlier. The bearing operating characteristics that have been under consideration in this paper were evaluated in the following manner.

Load carrying capacity

The force acting on the area between any four adjacent nodes is found by multiplying the averaged pressure by the area. This force was then resolved into components which were perpendicular and parallel to the line connecting the positions of maximum and minimum film thicknesses. In terms of the finite difference notation used, the components are

Parallel

$$P=\sum_{j=1}^{j=m-1}\sum_{i=1}^{i=n-1}\left\{\frac{p_{i,j}+p_{i,j+1}+p_{i+1,j}+p_{i+1,j+1}}{4}\right\}\Delta_i\Delta_j\cos\frac{x}{R_1}. \tag{18}$$

Perpendicular

$$V=\sum_{j=1}^{j=m-1}\sum_{i=1}^{i=n-1}\left\{\frac{p_{i,j}+p_{i,j+1}+p_{i+1,j}+p_{i+1,j+1}}{4}\right\}\Delta_i\Delta_j\sin\frac{x}{R_1}, \tag{19}$$

where x is measured from the datum to the centre of the enclosed area.

The load on the bearing is then given by

$$W=\sqrt{(P^2+V^2)}$$

Altitude angle

This can be found by the following equation:

$$\psi = \pi - \frac{x_1}{R_1} - \frac{1}{2}\left[\frac{x_2 - x_1}{R_1}\right] = \tan^{-1}\frac{V}{P}. \tag{20}$$

Power loss

The torque was assessed in a manner similar to that employed in calculating the load. The shear force acting on the area between the nodes is the average of the shear stresses multiplied by the enclosed area. The pressure gradient multiplied by the local lubricant film thickness at each node multiplied by the enclosed area is added to this. Hence the expression for the power loss is given by

$$H = \frac{UR_1}{4}\sum_{i=1}^{i=n'}\sum_{j=1}^{j=m}\{X_{i,j} + X_{i,j+1} + X_{i+1,j} + X_{i+1,j+1}\}\Delta_i\Delta_j, \tag{21}$$

where

$$X = T_i + \frac{h(x,z)}{2}\frac{\partial p}{\partial x}.$$

The pressure gradient over the greater part of the domain is evaluated using central differences. At $i = 1$ and $i = n'$ the position where $p = 0$ since $p < 0$ forward and backward differences were used as appropriate.

REFERENCES

1. S. Asanabe, M. Akahoshi and R. Asai, 'Theoretical and experimental investigation on misaligned journal bearing performance', *Paper C36/71, Tribology Convention 1971, Proc. Inst. Mech. Engrs.*, 1972.
2. O. Pinkus and S. S. Bupara, 'Analysis of misaligned grooved journal bearings', *Trans ASME, Journal of Lubrication Technology*, **101**, 503 (1979).
3. A. J. Smalley and H. McCallian, 'The effect of journal misalignment and the performance of a journal bearing under steady running conditions', *Proc. Inst. Mech. Engrs.*, **181** (Part 3B), 45 (1966–67).
4. M. J. Brann, R. L. Mullen and R. C. Hendricks, 'An analysis of temperature effect in a finite journal bearing with spatial tilt and viscous dissipation', *Trans. ASLE*, **27**, (4), 405 (1984).
5. C. W. Ng and C. H. T. Pan, 'A linearised turbulent lubrication theory', *Trans. ASME, J. Basic. Eng.*, **87**, (4), 675 (1965).
6. F. A. Martin and D. R. Garner, 'Plain journal bearings under steady loads: design guidance for safe operation', *Paper C313/73, Proc. Inst. Mech. Engrs.*, (1974).